Influence of GaAs/AlGaAs heterojunction on the photoemission properties of GaAs photocathode: a first-principles research

XIAOHUA YU[1,2,*], ZUDE JIN[1], HUIXIA SUN[1]
[1]*Department of Physics and Electronic Engineering, Yuncheng University, Yuncheng 044000, China*
[2]*Laboratory of Optoelectronic Information Science and Technology of Shanxi Province, Yuncheng 044000, China*

The electronic structure and optical properties of GaAs/$Al_{0.4}Ga_{0.6}As$ and GaAs/AlAs are studied by the first-principles method. The influence of heterojunction on GaAs photocathode is analyzed. Results show that the stability of heterojunction is lower than pure GaAs. The band bending at the interface is favorable for the flow of carriers toward the emitter layer. Electronic state localization is improved in heterojunction. The photon excitation energy region is located at 1.424~4.732 eV, in this region, the absorption coefficient of heterojunction is lower while the reflectivity of which is higher. The influence of GaAs/AlAs on photocathode is more obvious than that of GaAs/$Al_{0.4}Ga_{0.6}As$.

(Received May 30, 2023; accepted December 4, 2023)

Keywords: Heterojunction, First-principles, Electronic structure, Optical properties.

1. Introduction

With direct bandgap, GaAs materials have many excellent properties and have a wide application prospect in the fields of low-light night vision [1], solar cells [2], optical communication [3], quantum communication [4] and so on. With high sensitivity, small dark emission, concentrated emission electron energy distribution and high quantum efficiency, NEA (Negative Electron Affinity) GaAs photocathodes have a wide application prospect in the field of weak detection [5]. In 2010, Schwede et al. found a new solar energy conversion mechanism of PETE (Photo-Enhanced Thermionic Emission), of which the predicted total efficiencies can reach over 50%. NEA GaAs photocathodes are good candidates for PETE devices [6]. GaAs/AlGaAs heterojunction is indispensable in NEA GaAs photocathodes and has important application prospects in the laser and optical communication field [7]. In this paper, the first-principles method [8,9] was used to analyze the electronic properties and optical properties of GaAs/AlGaAs heterojunction, and the influence of heterojunction on photoemission of GaAs photocathode is researched.

2. Calculation models and calculation results

The calculation is implemented by the CASTEP software package, using the Perdew-Burke-Ernzerhof (PBE) functional, generalized gradient approximation (GGA) [8-10] is used to treat the exchange and correlation interactions. Norm-conserving is used to describe the wave function of the valence electron, which is chosen as: Ga:$3d^{10}4s^24p^1$, Al:$3s^23p^1$, As:$4s^24p^3$. The cutoff energy is chosen as 600 eV and the k-point mesh is 5×5×1, the convergence standard of single atom energy, inter-atomic interaction force, the stress in the crystal, and the maximum atomic displacement were set as 1.0×10^{-5} eV/Atom, 0.05 eV/Å, 0.05 Gpa and 0.002 Å respectively.

In GaAs/AlGaAs heterojunction models, there are 10 GaAs unit cells and 10AlGaAs unit cells, the Al content is chosen as 0.4 and 1. The model can be labeled as GaAs/$Al_{0.4}Ga_{0.4}As$ and GaAs/AlAs. For comparison, bulk models with 20 GaAs unit cells, 20 AlAs unit cells and 20 $Al_{0.4}Ga_{0.4}As$ unit cells are built, surface models of Ga-up GaAs(001), As-up $Al_{0.4}Ga_{0.4}As$ (001) and As-up AsAl(001) are built, they are labeled as pure-GaAs, pure-AlAs, pure-$Al_{0.4}Ga_{0.6}As$, GaAs-sur, $Al_{0.4}Ga_{0.4}As$-sur and AlAs-sur. The models are collected in Fig. 1.

3. Results

3.1. Surface energy and formation energy

Surface energy and formation energy can be used to analyze the stability of the heterojunction, they can be calculated through the following formulas [11,12]:

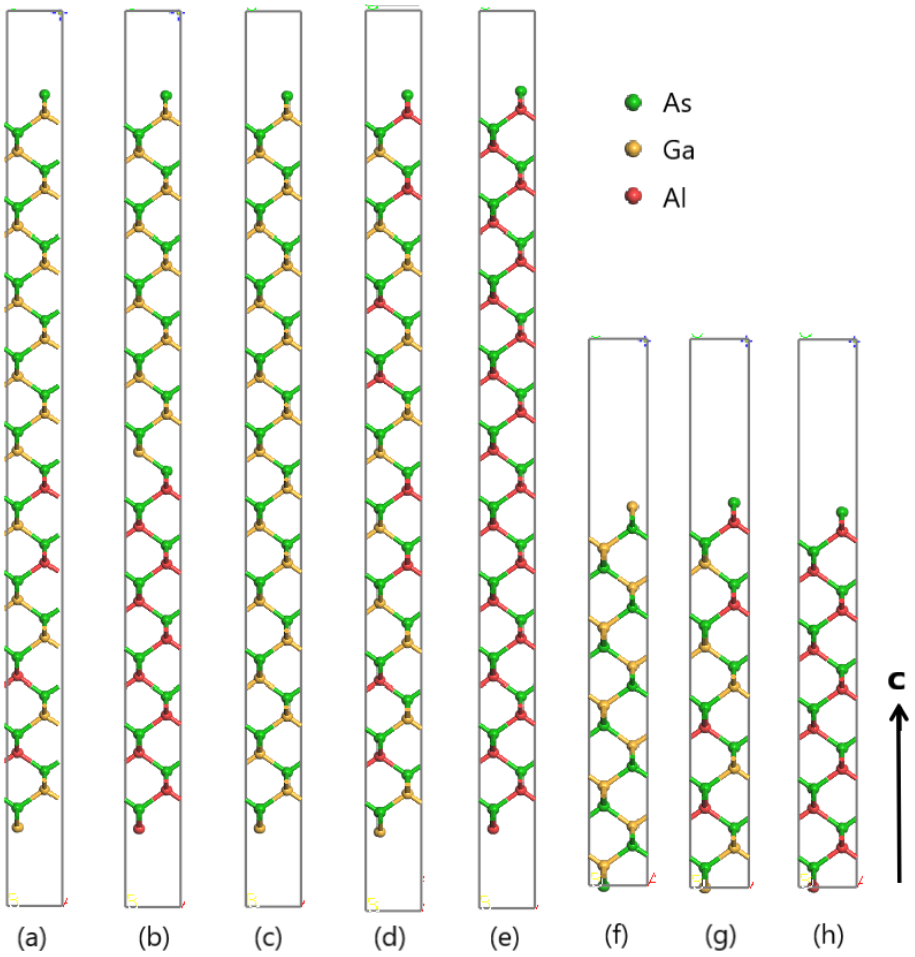

Fig. 1. The calculation models. (a),(b),(c),(d),(e),(f),(g) and (h) are respectively the model of GaAs/$Al_{0.4}Ga_{0.4}As$, GaAs/AlAs, pure-GaAs, pure-$Al_{0.4}Ga_{0.4}As$, pure-AlAs, GaAs-sur, $Al_{0.4}Ga_{0.4}As$-sur and AlAs-sur (color online)

$$E_{surface} = E_{total} - nE_{GaAs} - mE_{AlAs}$$
$$E_{form} = E_{total} - \frac{1}{2}E_{Pur-GaAs} - \frac{1}{2}E_{Pur-AlAs}(or E_{Pur-Al0.4Ga0.6As}) \quad (1)$$

where E_{total} means the total energy of the heterojunction models, E_{GaAs} and E_{AlAs} indicate the energy of GaAs and AlAs unit cells respectively. n and m are the number of GaAs and AlAs unit cell in heterojunction models respectively. $E_{Pur-GaAs}$, $E_{Pur-Al0.4Ga0.6As}$ and $E_{Pur-AlAs}$ mean the total energy of these models. The calculated surface energy and formation energy are shown in Table 1. Positive surface energy means that the stability of GaAs/$Al_{0.4}Ga_{0.6}As$ and GaAs/AlAs are lower than pure material. The formation energy of GaAs/$Al_{0.4}Ga_{0.6}As$ is negative, meaning that the formation of GaAs/$Al_{0.4}Ga_{0.6}As$ is exothermic and GaAs/$Al_{0.4}Ga_{0.6}As$ is stable. The formation energy of GaAs/AlAs is a little positive value, meaning that the formation of GaAs/$Al_{0.4}Ga_{0.6}As$ is slightly endothermic and GaAs/$Al_{0.4}Ga_{0.6}As$ is slightly unstable. Both $E_{surface}$ and E_{form} of GaAs/$Al_{0.4}Ga_{0.6}As$ are lower than GaAs/AlAs, meaning that the stability of GaAs/$Al_{0.4}Ga_{0.6}As$ is higher.

Table 1. Surface energy and formation energy of heterojunction models

	$GaAs/Al_{0.4}Ga_{0.6}As$	GaAs/AlAs
$E_{surface}$ (eV)	1.864	3.077
E_{form} (eV)	-0.142	0.022

Fig. 2 and Fig. 3 depict the electron density difference and band structure of $GaAs/Al_{0.4}Ga_{0.6}As$ and GaAs/AlAs. (c) of Fig. 2 and Fig. 3 show the band structure of GaAs, AlAs, and $Al_{0.4}Ga_{0.6}As$. In which the band gap of $Al_xGa_{1-x}As$ is calculated by the following formula [13]:

$$E_g(x) = \begin{cases} 1.424 + 1.247xeV \ldots\ldots\ldots\ldots\ldots x < 0.45 \\ 1.9 + 0.125x + 0.143x^2 \ldots\ldots\ldots x > 0.45 \end{cases} \quad (2)$$

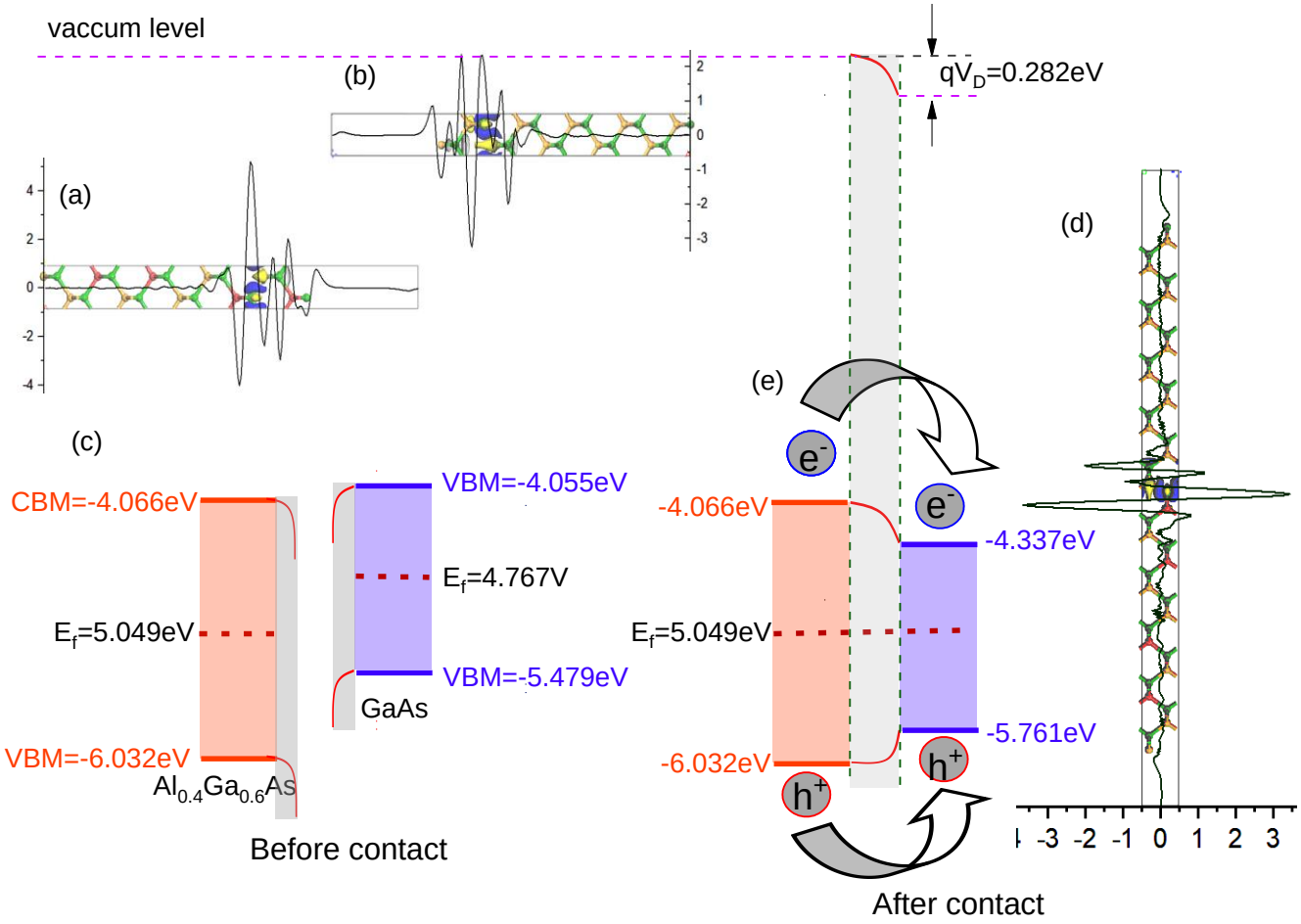

Fig. 2. (a) Electron density difference of GaAs surface. (b) Electron density difference of $Al_{0.4}Ga_{0.6}As$ surface. (c) Band structure of GaAs and $Al_{0.4}Ga_{0.6}As$ surface. (d) Electron density difference of $GaAs/Al_{0.4}Ga_{0.6}As$ heterojunction. (e) Band Structure of GaAs and $Al_{0.4}Ga_{0.6}As$ heterojunction. In (a), (b) and (d), electron density difference is shown by blue and yellow isoenergetic surface, blue means increase while yellow means decrease (color online)

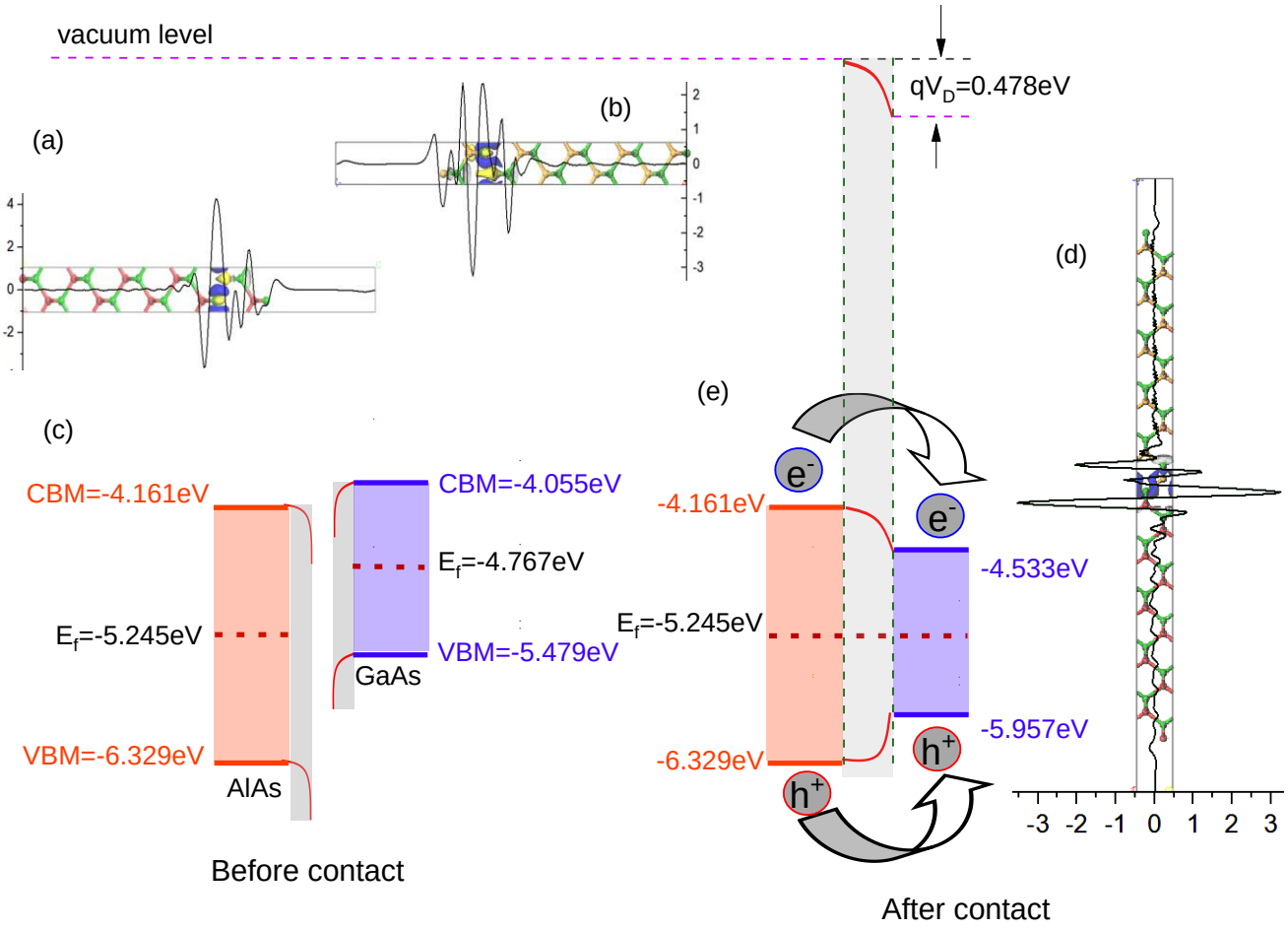

Fig. 3. (a) Electron density difference of GaAs surface. (b) Electron density difference of AlAs surface. (c) Band structure of GaAs and AlAs surface. (d) Electron density difference of GaAs/AlAs heterojunction.(e) Band Structure of GaAs and AlAs heterojunction. In (a),(b) and (d), electron density difference is shown by blue and yellow isoenergetic surface, blue means increase while yellow means decrease (color online)

3.2. Work function, band structure and density of state

The band gap of GaAs, $Al_{0.4}Ga_{0.6}As$ and AlAs are 1.424 eV, 1.966 eV and 2.168 respectively. GaAs has a direct bandgap, AlAs has an indirect bandgap, when the aluminum component is 0.45, the bandgap of GaAlAs turn from direct to indirect. The bandgap of GaAs, $Al_{0.4}Ga_{0.6}A$ is direct bandgap of Γ -valley while the bandgap of AlAs is an indirect bandgap of the *X*-valley. The work function Φ, defined as the minimum energy the electron need to escape from the materials, is equal to the difference between vacuum level and Fermi level [14]. The calculated work function of GaAs, $Al_{0.4}Ga_{0.6}As$ and AlAs are 4.767eV, 5.046eV and 5.245eV, the calculated values are consistent with the experimental results [15], showing the reliability of the calculated results. In Fig. 1 and Fig. 2 the vacuum level is defined as 0 eV, thus the positions of Fermi level of GaAs, $Al_{0.4}Ga_{0.6}As$ and AlAs are -4.767 eV, -5.046 eV and -5.245 eV respectively. Since the Fermi level of the intrinsic semiconductor is located in the center of the valence band maximum (VBM) and conduction band minimum (CBM), the location of VBM and CBM can be determined. (a), (b) of Fig. 2 and Fig. 3 show the electron density difference along the c-axis during the formation of the surface, positive value means the increase of electron density during the formation of the surfaces while negative value means the decrease of electron density. Results show that during the formation of AlAs surface and $Al_{0.4}Ga_{0.6}As$ surface, the electrons at the outermost As atom move towards the bulk, the electrons at the outermost two atom bilayer are decreased, and the electron of As at the third atom bilayer are increased obviously. During the formation of the GaAs surface, the electrons at the outermost bilayer are decreased and the electrons at the second bilayer are increased. During the formation of the surface, electrons at the surface move towards the bulk, showing n-type property and leading to a downward band bending region.

(d) of Fig. 2 and Fig. 3 show the electron density difference along the c-axis during the formation of the heterojunction, the electron transfer occurs primarily at the two atom bilayers at the interface. The electrons of

Ga of GaAs move toward the As atom of $Al_{0.4}Ga_{0.6}As$ and AlAs. The electron transfer at AlAs ($Al_{0.4}Ga_{0.6}As$) is more obvious than that of GaAs. During the formation of the heterojunction, the Fermi level should be uniform, thus the vacuum level, VBM and CBM of GaAs are pulled down. At the interface, the CBM of GaAs is lower than $Al_{0.4}Ga_{0.6}As$ and AlAs, which can promote the photoelectrons move to GaAs (emission layer), the VBM of GaAs is higher than $Al_{0.4}Ga_{0.6}As$ and AlAs, which can promote the hole move towards GaAs. The band bending at the interface of the heterojunction is favorable for the flow of carriers towards the emitter layer (GaAs).

The band structure and DOS curves of $GaAs/Al_{0.4}Ga_{0.6}As$ and GaAs/AlAs are calculated and collected in Fig. 4 and Fig. 5. Since the electron transfer mainly occurs at the interface, the DOS curves focus on two GaAs unit cells and two $Al_{0.4}Ga_{0.6}As$ (or AlAs) unit cells at the interface, to facilitate data comparison, the results are the average value from every unit cells. The average DOS of pure GaAs and $Al_{0.4}Ga_{0.6}As$ (or AlAs) are contained for comparison. The calculated band gap of GaAs is 0.793 eV and the experiment band gap of GaAs is 1.424 eV, the calculated band gap is underestimated, this is a common phenomenon in GGA calculation [16], some researchers try to use the algorithm of adding U to modify the energy band. However, the essence of the U value and the selection of the U value still need to be verified. Considering that the work function is consistent with the experimental value, adding U is not used in this manuscript. The calculated band gap of $GaAs/Al_{0.4}Ga_{0.6}As$ and GaAs/AlAs respectively 0.927 eV, 0.921 eV. The band gap of heterojunction is higher than pure GaAs.

In DOS curves, the Ga 3d state only contributes to the deep valence band located at about 16.5 eV, in the heterojunction the energy region of this deep valence band is narrowed, showing that the localization of this band is enhanced. Since the Ga 3d state does not contribute to other energy levels, it is not included in Fig. 4 and Fig. 5.

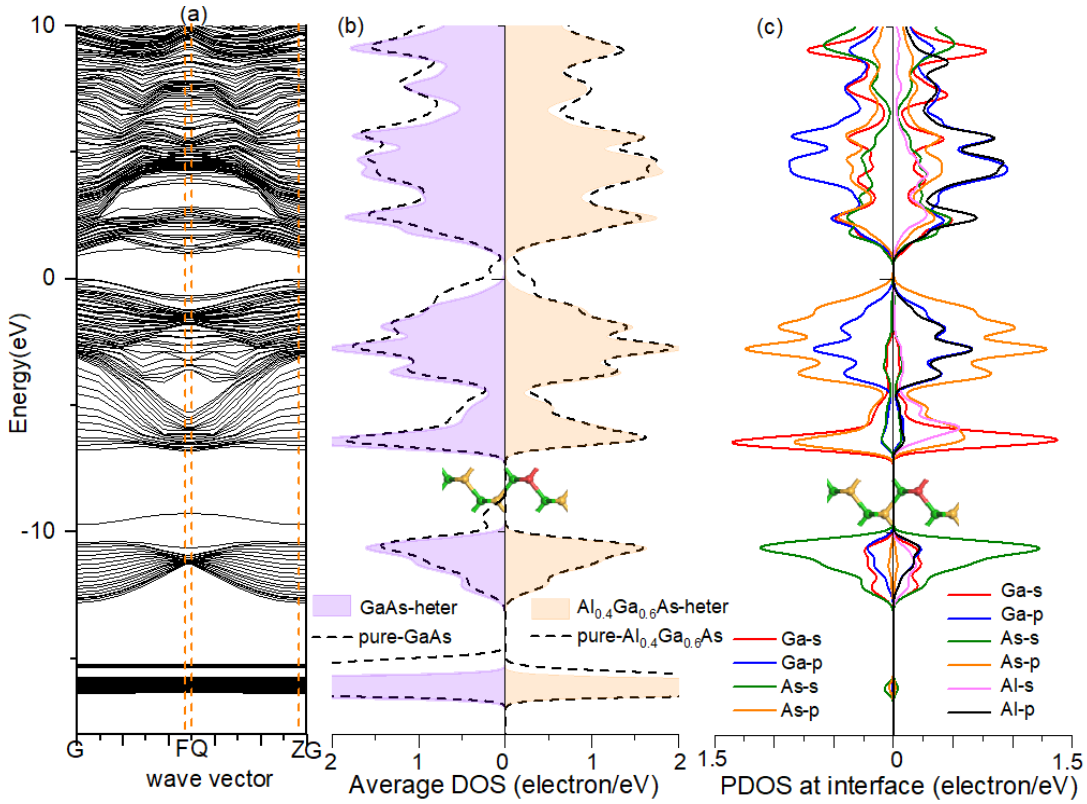

Fig. 4. DOS curves of $GaAs/Al_{0.4}Ga_{0.6}As$ heterojunction. (a) Band structure of $GaAs/Al_{0.4}Ga_{0.6}As$. (b) Average DOS of $GaAs/Al_{0.4}Ga_{0.6}As$, the left side shows the average DOS of two GaAs unit cells at the interface, and the right side shows the average DOS of two $Al_{0.4}Ga_{0.6}As$ unit cells at the interface. The dotted curves show the average DOS in pure GaAs and $Al_{0.4}Ga_{0.6}As$. (c) Partial DOS(PDOS) of GaAs/ $Al_{0.4}Ga_{0.6}As$, the left side shows the PDOS of two GaAs unit cells at the interface, and the right side shows the PDOS of two $Al_{0.4}Ga_{0.6}As$ unit cells at the interface (color online)

The valence band of $GaAs/Al_{0.4}Ga_{0.6}As$ contains an upper valence band located at -7.251~0 ev and a lower valence band located at 12.968~9.714 eV. Compared to pure GaAs, the energy regions of two valence band are narrowed and the localization is enhanced. Energy levels at the region of -4.502~0 eV mainly contain Ga 4p, Al 4p and Al 3p, the top of VBM is mainly determined by As 4p. The energy levels at the region of -7.251 ~ -4.502 eV

mainly contain Ga 4s, As 4p and Al 3s. The lower valence band is mainly contributed by As 4s state. On two sides of the interface, the difference of Ga atoms only appears at -7.251 ~ -4.502 eV. The conduction band contains all the states except Ga 3d. The DOS at the bottom of the CBM of GaAs/$Al_{0.4}Ga_{0.6}$As is higher than pure GaAs, which can promote photoelectric emission.

The DOS curve of GaAs/AlAs is rather similar to GaAs/$Al_{0.4}Ga_{0.6}$As, the difference is that the upper and lower valence bands of GaAs/AlAs are narrower than GaAs/$Al_{0.4}Ga_{0.6}$As, showing that the localization of GaAs/AlAs is more obvious. 4s and 4p of the Ga atoms are rather similar to 3s and 3p states of the Al atoms, the main difference between Ga state and Al state appears at -7.251 ~ -4.502 eV. The DOS improvement at the bottom of the CBM of GaAs/AlAs is more obvious than that of GaAs/$Al_{0.4}Ga_{0.6}$As.

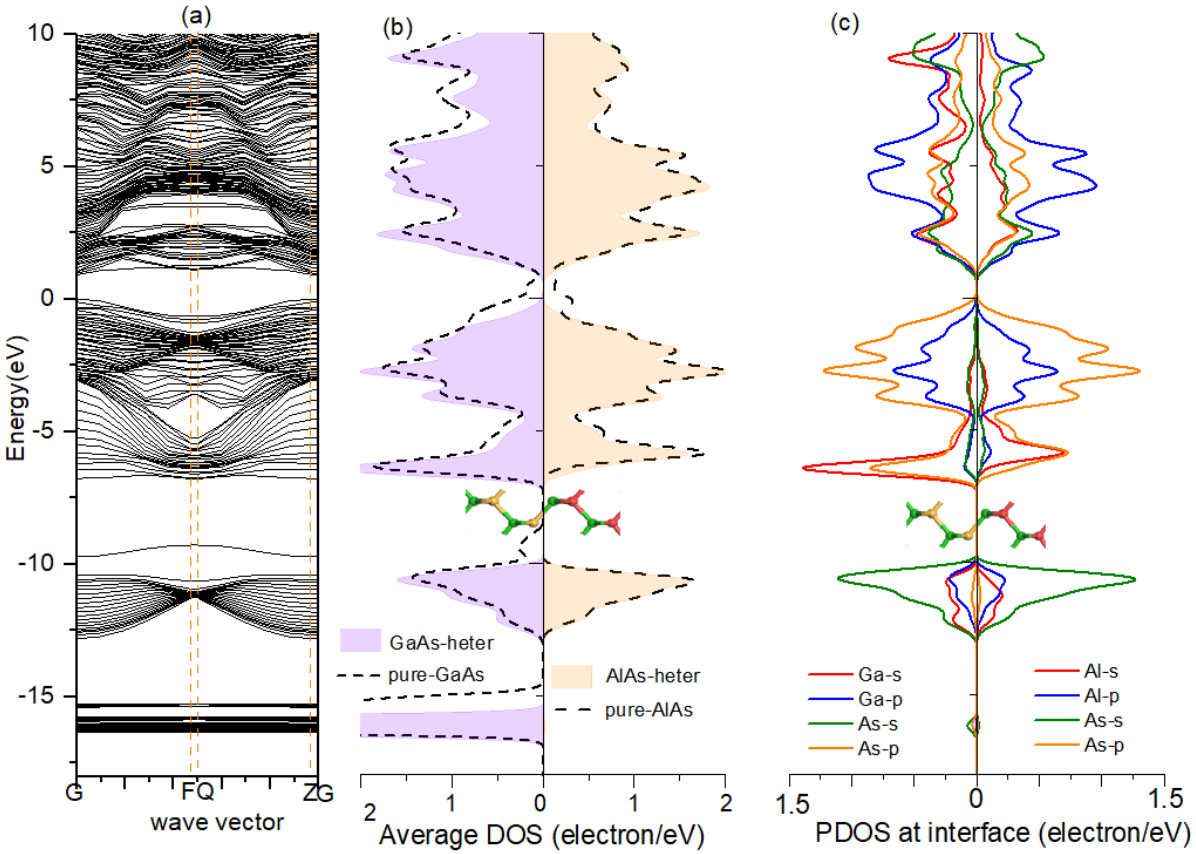

Fig. 5. DOS curves of GaAs/AlAs heterojunction (a) Band structure of GaAs/AlAs. (b) Average DOS of GaAs/AlAs, the left side shows the average DOS of two GaAs unit cells at the interface, and the right side shows the average DOS of two AlAs unit cells at the interface. The dotted curves show the average DOS in pure GaAs and AlAs. (c) Partial DOS(PDOS) of GaAs/AlAs, the left side shows the PDOS of two GaAs unit cells at the interface, and the right side shows the PDOS of two AlAs unit cells at the interface (color online)

3.3. Optical properties

According to Kramers–Kronig dispersion relations, the dielectric function $\varepsilon(\omega)=\varepsilon_1(\omega)+i\varepsilon_2(\omega)$ can be calculated by following formulas [17]:

$$\varepsilon_2(\omega)=\frac{\pi}{\varepsilon_0}\left(\frac{e}{m\omega}\right)^2\cdot\sum_{V,C}\left\{\int_{BZ}\frac{2dK}{(2\pi)^2}\left|a\cdot M_{V,C}\right|^2\delta[E_C(K)-E_V(K)-\hbar\omega]\right\} \tag{3}$$

$$\varepsilon_1(\omega)=1+\frac{2e}{\varepsilon_0 m^2}\cdot\sum_{V,C}\int_{BZ}\frac{2dK}{(2\pi)^2}\frac{\left|a\cdot M_{V,C}(K)\right|^2}{[E_C(K)-E_V(K)]/\hbar}\cdot\frac{1}{[E_C(K)-E_V(K)]^2/\hbar^2-\omega^2} \tag{4}$$

where C and V are respectively the conduction band and valence band, $E_C(K)$ and $E_V(K)$ are respectively the intrinsic energy level of the conduction band and valence band. BZ is the first Brillouin zone, K is the electron wave vector, a is the unit direction vector of the vector potential A, and $M_{V,C}$ is the transition matrix element. The calculated real part of dielectric function of GaAs/$Al_{0.4}Ga_{0.4}As$, GaAs/AlAs and pure-GaAs are shown in Fig. 6. Results show that the influence of heterojunction on GaAs is mainly in low energy region (0~6.712 eV), in the energy range of 4.732eV~14.561eV, $\varepsilon_1 < 0$, photons in this energy range cannot spread in the material, showing the metal reflection characteristics. Compared to pure GaAs, the metal reflection characteristic region of heterojunction slightly shrinks to the higher energy, the heterojunction of GaAs/AlAs is the smallest, the peak values in the metal reflection characteristic region of heterojunctions are higher and the peak value of GaAs/AlAs is the highest. In the region of 0~0.56 eV, the ε_1 relationship is GaAs>GaAs/$Al_{0.4}Ga_{0.4}As$>GaAs/AlAs.

On one hand, the photon with energy $E > 1.424eV$ can be adsorbed and inspire photoelectrons, on the other hand, the photon in metal reflection characteristic region cannot spread, as a result, the photoemission of GaAs mainly occurs at 1.424 eV~4.732 eV. In the region of 1.424 eV~2.214 eV, ε_1 of the heterojunction is lower than pure GaAs, ε_1 of GaAs/AlAs is lowest. In the region of 2.214 eV~4.732 eV, ε_1 of the heterojunction is higher than pure GaAs, ε_1 of GaAs/AlAs is highest.

The light absorption coefficient expresses the percentage of light intensity attenuation per unit of distance traveling in the medium. Absorption spectra can be obtained by:

$$\alpha \equiv 2\omega k / c = 4\pi k / \lambda_0 \tag{5}$$

where λ_0 is the wavelength of light in vacuum, ω is the angular frequency, k, the extinction coefficient, can be calculated by the following formula:

$$k^2 = \frac{1}{2}\left(\left(\varepsilon_1^2 + \varepsilon_2^2\right)^{\frac{1}{2}} - \varepsilon_1\right) \tag{6}$$

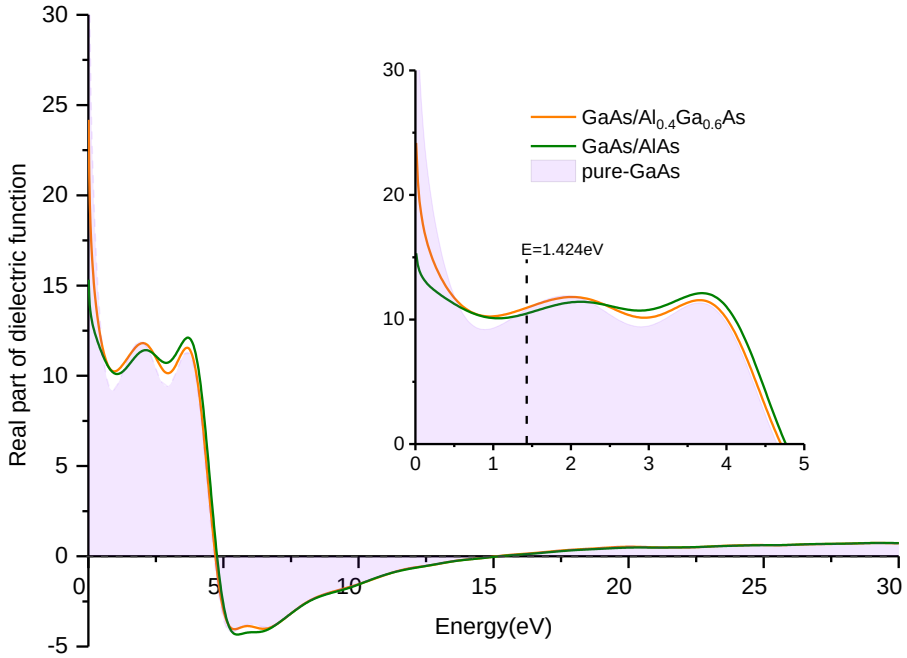

Fig. 6. Real part of the dielectric function of GaAs/$Al_{0.4}Ga_{0.4}As$, GaAs/AlAs and pur-GaAs (color online)

The calculated absorption coefficients of GaAs/$Al_{0.4}Ga_{0.4}As$, GaAs/AlAs and pure-GaAs are shown in Fig. 7. The absorption peaks of pure GaAs, which are labeled as P1~P11, located at 0.627 eV, 2.713 eV, 5.147 eV, 6.686 eV, 9.183 eV, 12.369 eV, 18.223 eV, 20.891 eV, 25.172 eV, 27.258 eV, 29.829 eV. In the heterojunction, P1 and absorption peaks located at high energy region (P7~P11) move towards lower energy side and the peak values are decreased, P4 moves to the lower energy side and the peak value is increased, P2 and P6 almost disappeared, P3 and P5 move to the high energy side and the peak values are increased. In the photon excitation energy region of 1.424 eV~4.732 eV, the absorption coefficient of the heterojunction is lower than GaAs. The influence of GaAs/$Al_{0.4}Ga_{0.4}As$ on absorption is more obvious than GaAs/AlAs.

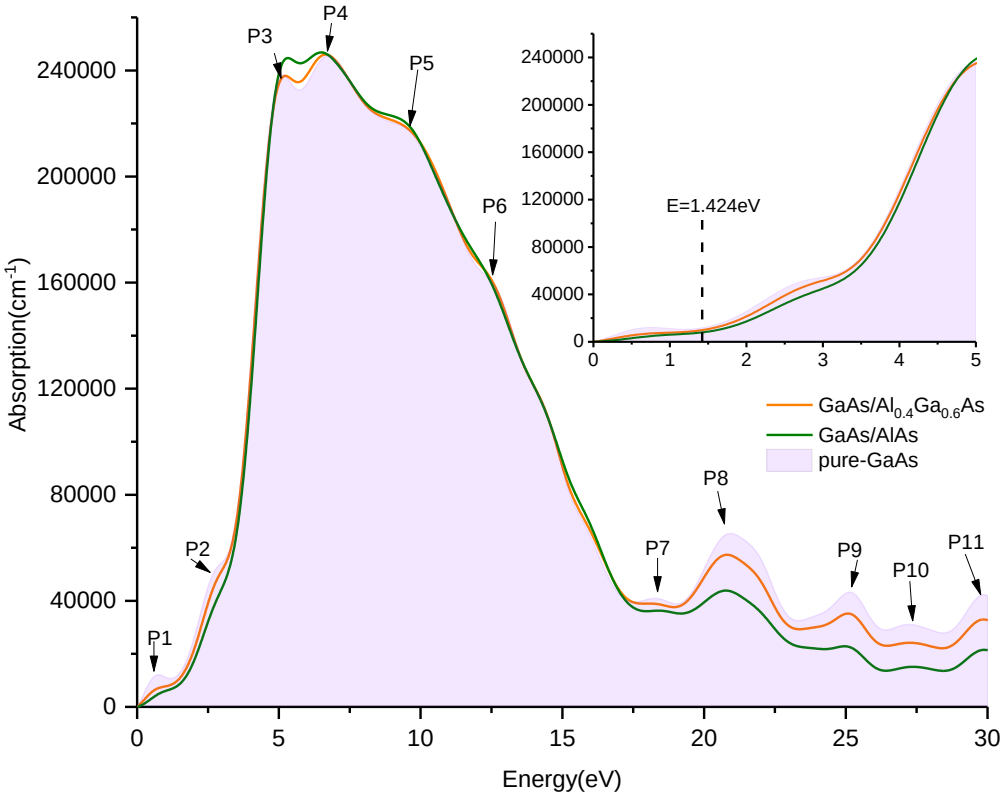

Fig. 7. Absorption of GaAs/$Al_{0.4}Ga_{0.4}As$, GaAs/AlAs and pur-GaAs (color online)

Reflectivity can be calculated as the following formula:

$$R(\omega)=[(n-1)^2+k^2]/[(n+1)^2+k^2] \quad (7)$$

where n is the refractive index and can be determined by:

$$n^2=\frac{1}{2}\left(\left(\varepsilon_1^2+\varepsilon_2^2\right)^{\frac{1}{2}}+\varepsilon_1\right) \quad (8)$$

The calculated reflectivity of GaAs/$Al_{0.4}Ga_{0.4}As$, GaAs/AlAs and pure-GaAs are shown in Fig. 8. In the region of 0~2.933 eV, heterojunction causes the decrease of reflectivity. In the region of 5.209~21.296 eV, heterojunction causing the increase of reflectivity. In the other energy region, the reflectivity almost remains unchanged. In the photon excitation energy region of 1.424~4.732 eV, the reflectivity of heterojunction is lower than pure GaAs. The influence of GaAs/$Al_{0.4}Ga_{0.4}As$ on absorption is more obvious than GaAs/AlAs.

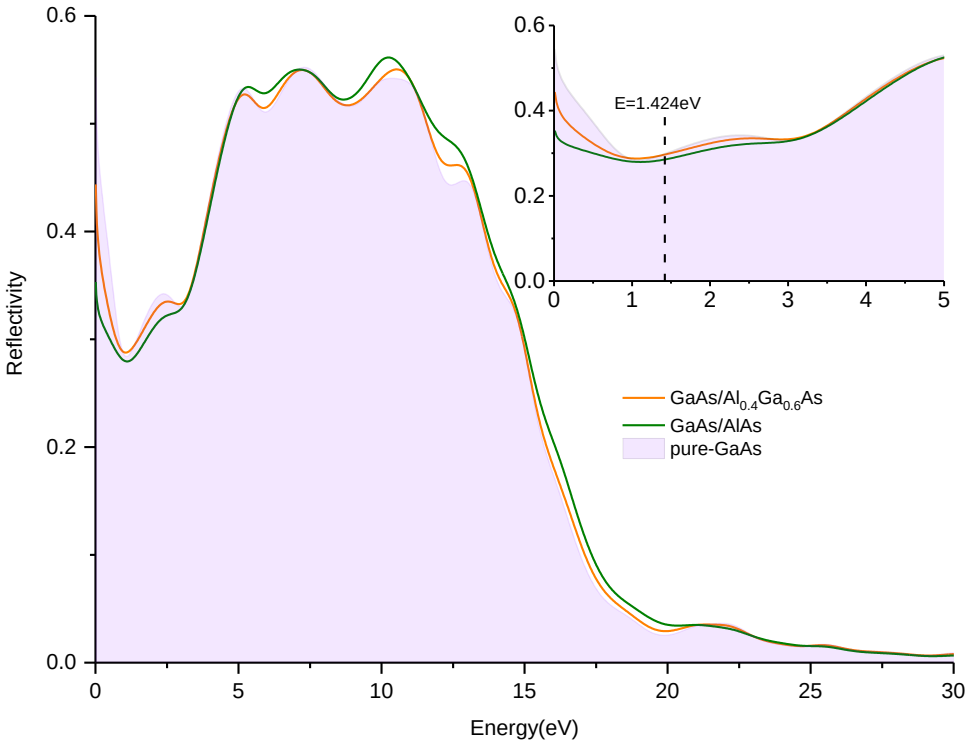

Fig. 8. Reflectivity of GaAs/$Al_{0.4}Ga_{0.4}As$, GaAs/AlAs and pur-GaAs (color online)

4. Conclusion

In this letter, the electronic structure and optical properties of two GaAs/AlGaAs heterojunctions (GaAs/$Al_{0.4}Ga_{0.6}As$ and GaAs/AlAs) are studied by the first-principles method. The influence of heterojunction on GaAs photocathode is analyzed. Results show that the stability of heterojunction is lower than pure GaAs. GaAs/$Al_{0.4}Ga_{0.6}As$ is stable while GaAs/$Al_{0.4}Ga_{0.6}As$ is slightly unstable. At the interface, the CBM of GaAs is lower than $Al_{0.4}Ga_{0.6}As$ and AlAs, the VBM of GaAs is higher than $Al_{0.4}Ga_{0.6}As$ and AlAs, the band bending at the interface of the heterojunction is favorable for the flow of carriers towards the emitter layer (GaAs). The DOS at the bottom of CBM in heterojunctions is higher than pure GaAs, which can promote photoelectric emission. Dielectric function results show that photoemission of GaAs mainly occurs at 1.424 eV~4.732 eV, in this region the absorption coefficient of heterojunction is slightly lower than GaAs while the reflectivity of heterojunction is slightly higher than GaAs, which is unfavorable to photoelectric emission. The influence of GaAs/AlAs on photocathode is more obvious than that of GaAs/$Al_{0.4}Ga_{0.6}As$.

Acknowledgement

This work is supported by the Scientific and Technologial Innovation Programs of Higher Education Institutions in Shanxi (2022L472 and 2022L476).

References

[1] J. Zhang, Y. Zhang, Y. Qian, F. Shi, K. Zhang, G. Jiao, H. Cheng, X. Bai, Appl. Surf. Sci. **535**, 147691 (2021).
[2] A. Luque, A. Marti, C. Stanley, Nat. Photonics. **6**, 146 (2012).
[3] R. M. Balagula, M. Jansson, M. Yukimune, J. E. Stehr, F. Ishikawa, W. M. Chen, I. A. Buyanova, Sci. Rep. **10**, 8216 (2020).
[4] S. Manna, H. Huang, S. F. C. D. Silva, C. Schimpf, M. B. Rota, B. Lehner, M. Reindl, R. Trotta, A. Rastelli, Appl. Surf. Sci. **532**, 147360 (2020).
[5] Y. Zhang, B. Chang, J. Zhao, F. Shi, H. Cheng, Appl. Phys. Lett. **99**, 101104 (2011).
[6] Y. Diao, L. Liu, S. Xia, Appl. Nanosci. **10**, 807 (2020).
[7] C. Feng, Y. Zhang, J. Liu, Y. Qian, X. Liu, F. Shi, H. Cheng, Appl. Opt. **56**, 9044 (2017).
[8] X. Yu, Z. Jin, F. Liu, G. Shao, H. Sun, Optoelectron. Adv. Mat. **15**(11-12), 607 (2021).
[9] J. Guo, Y. Li, Optoelectron. Adv. Mat. **17**(1-2), 8 (2023).
[10] J. Perdew, K. Burke, M. Ernzerhof, Phys. Rev. Lett. **77**, 3865 (1996).
[11] G. G. Xu, Q. Y. Wu, J. M. Zhang, Z. G. Chen, Z. G. Huang, Acta Physica Sinica **58**, 1924 (2009).

[12] Y. J. Du, B. K. Chang, J. J. Zhang, B. Li, X. H. Wang, Acta Physica Sinica **61**, 067101 (2012).
[13] X. Yu, Z. Ge, B. Chang, M. Wang, H. Wang, Optik **125**, 587 (2014).
[14] A. L. Rosa, J. Neugebauer, Phys. Rev. B. **732**, 05346 (2006).
[15] N. Inoue, T. Higashino, K. Tanahashi, Y. Kawamura, J. Cryst. Growth **227**, 123 (2001).
[16] W. E. Pickett, Comput. Phys. Rep. **9**, 115 (1989).
[17] Q. Chen, Q. Xie, W. J. Yan, Sci. China (Ser. G) **38**, 825 (2008).

*Corresponding author: 624554818@qq.com